Particle in a Horizontally shaken Box: Particle in a Horizontally Shaken Box: Period-Doubling, Chaos, and Chattering

Barbara Drossel and Thomas Prellberg

Department of Theoretical Physics, University of Manchester
Manchester M13 9PL, United Kingdom
E-mail: drossel@a13.ph.man.ac.uk, prel@a13.ph.man.ac.uk

Abstract. We study the dynamics of a particle in a horizontally and periodically shaken box as a function of the box parameters and the coefficient of restitution. For certain parameter values and initial conditions, the particle becomes regularly chattered at one of the walls, thereby loosing all its kinetic energy relative to that wall. The number of container oscillations between two chattering events depends in a fractal manner on the parameters of the system. Alternatively, the particle can become trapped on a periodic orbit and follow the period–doubling route to chaos when the coefficient of restitution is changed. The basins of attraction of different orbits are strongly interwoven.

1 Introduction and Summary

While vertically shaken granular materials have been the object of intensive research in the past years, the investigation of horizontally shaken granular materials has just started [1, 2]. Vertically shaken materials show various cellular patterns and localized oscillons [3, 4, 5], and their horizontal counterpart was recently found to display ripple–like patterns [1]. Since these patterns are due to the collective behaviour of many interacting particles, the one–particle system shows completely different phenomena that are, however, equally fascinating. The dynamical evolution of a bouncing ball on a vibrating platform was studied extensively [6, 7, 8]. As long as the coefficient of restitution is smaller than one, a particle that hits the platform with sufficiently small relative velocity bounces off the platform infinitely often during a finite time and looses its memory of earlier dynamics. Luck and Mehta [8] argue that this "chattering" is the fate of generic trajectories, which therefore become periodic. They conclude that true chaos cannot be observed in this system. Other authors, however, find that a trajectory can become trapped on a strange attractor with a nonvanishing probability [9].

In this article, we study the dynamics of a singe particle in a horizontally shaken box. While chattering occurs for part of the parameter values and initial conditions, we find as well other generic scenarios like periodic orbits without chatter, the period–doubling route to chaos, and strange attractors. The interplay between these different modes of behaviour makes this apparently simple

system astonishingly rich and fascinating. The main results of this article have been published earlier [10].

The outline of this article is as follows: In the next section we define the system used in our simulations. In Section 3 we discuss the limiting case of a completely inelastic particle that assumes the velocity of the wall at each collision. When the particle hits the wall during the half period where the wall accelerates toward it, it sticks to the wall until the end of the half period. The number of reflections until this locking occurs depends in a fractal manner on the parameter of the system. The physically more relevant case of a partially elastic particle is then studied in Section 4. Increasing the coefficient of restitution from zero, the period–doubling route to chaos is observed in many cases. Ultimately, the strange attractor becomes so large that it includes the chattering region, thus making the orbits again periodic. Whether a trajectory starting in the chattering region leads back to it, depends sensibly on the parameters, since basins of attraction of different orbits are strongly interwoven. Section 5 concludes the article.

2 The Model

The left and right wall of a horizontally shaken container of length L are described by the equations

$$\begin{aligned} x_{\text{leftwall}} &= A\sin(\omega t) \\ x_{\text{rightwall}} &= L + A\sin(\omega t)\,. \end{aligned}$$

ω is the frequency, and A the amplitude of shaking. We denote position and velocity of the particle by x and v respectively, and introduce the relative position and velocity with respect to the container walls

$$l = x - A\sin(\omega t) \quad , \quad u = v - A\omega\cos(\omega t)\,. \tag{1}$$

Between collisions, the particle moves with constant velocity. (The influence of friction between the particle and the container bottom will be discussed shortly in the conclusion.)

The collisions with the wall are partially inelastic, and the relative velocity u changes according to

$$u' = -\eta u \tag{2}$$

at each collision, where η is the coefficient of restitution.

It is convenient to measure the particle position in units of the amplitude A, time in units of the inverse frequency ω^{-1}, and velocity in units of $A\omega$. Then the system can be described by the dimensionless parameters $\alpha = L/A$, and η. We denote the dimensionless time, length, and velocity again by t, l, and u. We also introduce the phase of the container oscillation $\phi = \omega t \bmod 2\pi$.

The motion of the particle can be written down immediately. It is customary to describe the particle dynamics in terms of a map that gives the phase of the

container oscillation and the particle velocity immediately after an impact as function of their values immediately after the previous impact. Let the particle leave the left wall ($l = 0$) after an impact at $t = t_0$ with a relative velocity u_0. The particle moves according to

$$l_{t_0,u_0}(t) = \sin t_0 - \sin t + (u_0 + \cos t_0)(t - t_0) \,, \tag{3}$$

the corresponding velocity being $u = dl/dt$. The next collision occurs at the smallest solution $t_c > t_0$ of

$$l_{t_0,u_0}(t_c) = 0 \qquad \text{impact at same wall} \tag{4a}$$

$$l_{t_0,u_0}(t_c) = \alpha \qquad \text{impact at other wall} \tag{4b}$$

at which the velocity is $u_c = u_{t_0,u_0}(t_c)$. If the particle impacts again the same wall, the new velocity is now $u_1 = -\eta u_c$. On the other hand, if the particle collides with the right wall, it is convenient to use the symmetry between left and right wall to map the right wall to the left wall via $t \to t - \pi$ and $l \to \alpha - l$, so that now $u_1 = \eta u_c$. The velocity is thus always measured with respect to the wall at which the last impact has occurred.

Given an initial phase $\phi_0 = t_0$ and velocity u_0, we thus arrive at the map

$$\phi_1 = t_c \bmod 2\pi \,, \quad u_1 = -\eta u_c$$
$$\text{impact at same wall} \tag{5a}$$

$$\phi_1 = (t_c - \pi) \bmod 2\pi \,, \quad u_1 = \eta u_c$$
$$\text{impact at other wall} \tag{5b}$$

3 The Completely Inelastic Particle

3.1 Modelling by a One-Dimensional Map

We now discuss the case $\eta = 0$ in detail. The particle moves freely between the walls, and after an impact the relative velocity u_0 with respect to the wall is zero. This means that the two–dimensional mapping defined above is in fact reduced to a one-dimensional mapping. The subsequent fate of the particle depends only on the phase ϕ_0 at the moment of impact.

For $\phi_0 \in [0, \pi/2[\bmod 2\pi$, the particle is reflected from the wall with (absolute) velocity $\cos(\phi_0)$ and is headed for the other wall. For $\phi_0 \in [\pi, 2\pi[\bmod 2\pi$, the particle sticks to the wall until $\phi_0 = 2\pi$, and then leaves the wall with (absolute) velocity 1. In the intermediate region $\phi_0 \in]\pi/2, \pi[\bmod 2\pi$, the sign of the particle velocity is not reversed during the collision, and the particle hits the same wall again at a later phase ϕ_1 which is determined by the Equations (3), (4a), and (5a), leading to

$$\sin \phi_0 - \sin \phi_1 + (\phi_1 - \phi_0) \cos \phi_0 = 0 \,. \tag{6}$$

For $\phi_0 \geq \phi^c = 1.79..$, the phase ϕ_1 is in the locking interval $[\pi, 2\pi[$. As we are interested in the dynamics between impacts at opposite walls, we can extend

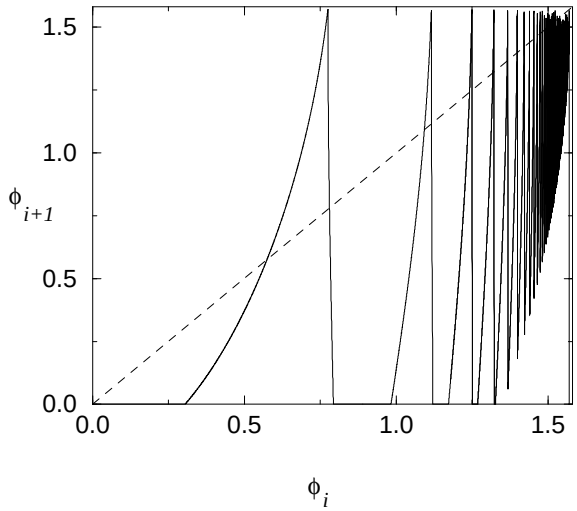

Fig. 1. The map for $\alpha = 9$.

the locking interval to include ϕ^c, i.e., to the interval $[\phi_c, 2\pi]$. For $\phi_0 < \phi^c$, the phase ϕ_1 is in the interval $[0, \pi/2[$ mod 2π and the particle is immediately reflected towards the other wall, where it arrives at a phase ϕ_2 now given by (4b) and (5b), i.e.,

$$\sin\phi_1 + \sin\phi_2 + (\phi_2 - \pi - \phi_1)\cos\phi_1 = \alpha\,. \tag{7}$$

From now on, let ϕ_i denote the phase of a wall at the moment where the particle is reflected towards the other wall for the ith time. We do not count reflections that lead to a subsequent reflection at the same wall. Then, the map that gives ϕ_{i+1} as function of ϕ_i is a map of the interval $[0, \pi/2[$ into itself, dependent only on the dimensionless parameter $\alpha = L/A$. The map $\phi_{i+1} = \Phi_\alpha(\phi_i)$ is given implicitly by Equations (6) and (7), and is shown in Fig. 1 for the value $\alpha = 9$. Branches with positive slope correspond to a particle arriving at the other wall at a phase in the interval $[0, \pi/2]$, from where it is immediately reflected back, while branches with negative slope indicate a twofold reflection at the other wall, the first reflection being in the phase interval $]\pi/2, \phi^c]$. For values of ϕ_i for which the particle hits the other wall in the locking region, the map has an horizontal branch with $\phi_{i+1} = 0$. The dashed line is the diagonal $\phi_{i+1} = \phi_i$. For $\pi/2 > \phi_i > \pi - \phi^c$, the velocity of the particle is so small that it cannot hit the other wall in the locking region. A small interval $\Delta\phi_i$ maps onto an interval $\Delta\phi_{i+1}$ proportional to the flight time, which is of the order $\alpha/\cos\phi_i$. For this reason, the density of branches in the map increases with increasing α and ϕ_i and diverges when ϕ_i approaches the value $\pi/2$, where the initial velocity decreases to zero.

3.2 Periodic Trajectories

The phase $\Phi_\alpha(0)$ at which a particle starting at phase zero will be reflected from the other wall depends on α. It is zero for $\alpha \in [(2n-1)\pi + \phi^c + \sin\phi^c, (2n+1)\pi]$, for any nonnegative integer n. In this case, a particle that starts in the locking region will hit the locking region at the other wall, and the periodicity of such a trajectory is one, as in Fig. 1. A period–doubling bifurcation sequence occurs when α is decreased below $(2n-1)\pi + \phi^c + \sin\phi^c$. In Fig. 2, this scenario is sketched. Since it involves only the first two branches of the map, the other branches are not shown. As soon as the map starts with a nonzero value, the period of a trajectory that starts in the locking region becomes two, as shown in Fig. 2 for $\alpha = 5.8$. With decreasing α, the endpoint of the trajectory moves to the right, and finally hits the foot of the second branch, leading to a second period–doubling bifurcation. For $\alpha = 5.743$, one observes therefore a cycle of period 4. When α is decreased further, the end point of the 4–cycle moves to the left and hits the foot of the first branch, leading to another period doubling. The last part of Fig. 2 shows an 8–cycle for $\alpha = 5.7406$. This period–doubling scenario continues as the end point of the 8–cycle moves to the left, etc., and the period becomes infinite when the trajectory hits the unstable fixed point on the first branch. For even smaller values of α, other periodicities are observed that are not powers of 2.

Fig. 2 shows also that the map intersects the vertical axis with a slope zero. This is true for any value of α, since the initial velocity does not change with ϕ_i for $\phi_i = 0$. For values α only slightly above $(2n+1)\pi$, the phase $\phi_{i+1}(0)$ is small, and the map intersects the diagonal $\phi_{i+1} = \phi_i$ with a positive slope smaller than one, leading to a stable fixed point $\phi^\star$ close to zero. This fixed point vanishes with increasing α via a saddle–node bifurcation, and for values of α slightly beyond the bifurcation, a particle trajectory can be trapped for a long time in the neighborhood of the former fixed point, before it escapes and hits ultimately the locking region where $\phi_{i+1} = 0$. When α increases further, the number of reflections in the neighborhood of the former fixed point (or, more precisely, on the first branch that has positive slope), decreases in steps of size one. Close to such a decrease, a trajectory that leaves the first branch goes through the upper right–hand corner of the map and can therefore have an arbitrarily large periodicity. Further away from it, a trajectory can hit the locking region immediately after leaving the first branch. In general, very complex trajectories can occur. In particular when $\Phi_\alpha(0)$ is close to $\pi/2$, the trajectory will spend some time in the upper right–hand corner of the map, and a slight change in α may lead to a large change in the periodicity of the trajectory. However, there exist no chaotic trajectories. Since the absolute value of the slope of the map is larger than one everywhere except for small phases, a small phase interval is stretched at each reflection, until in either hits the absorbing region, or becomes trapped in the region of small slope and attracted to a fixed point. In both cases, the trajectory becomes periodic.

Fig. 3 shows the period of a trajectory originally starting in the absorbing region as function of α. (There may exist other periodic orbits that do not

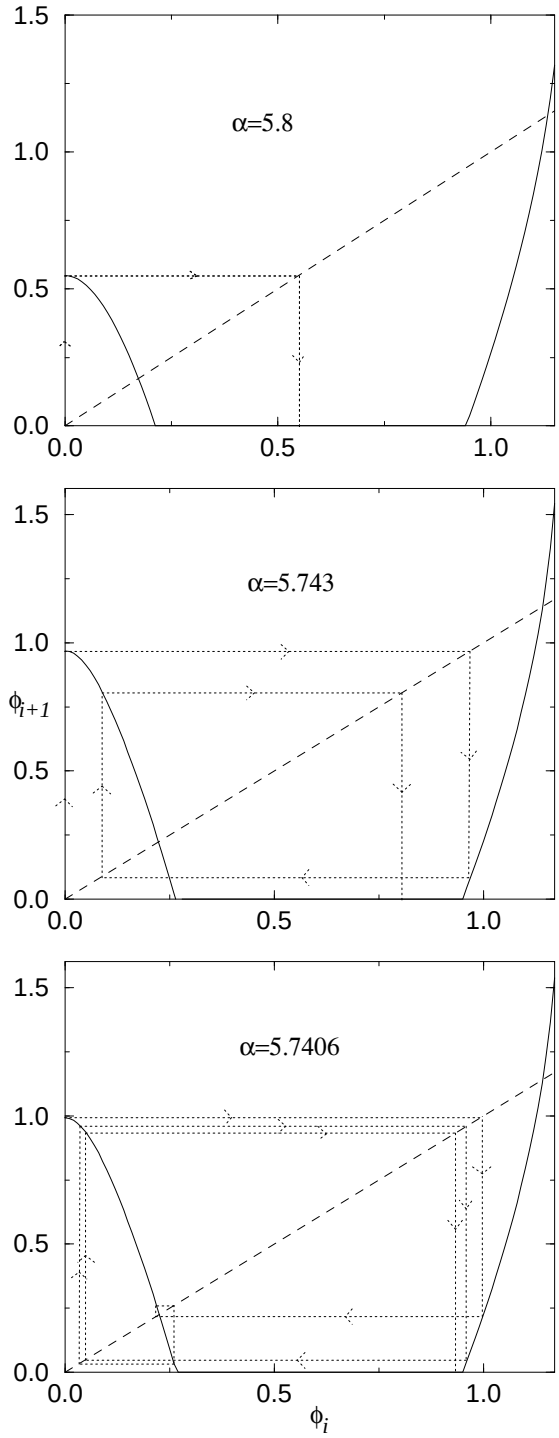

Fig. 2. A series of bifurcations when α is decreased.

go through the absorbing region and that coexist with the trajectories studied here.) All the above–mentioned features can be seen: the large plateaus of period

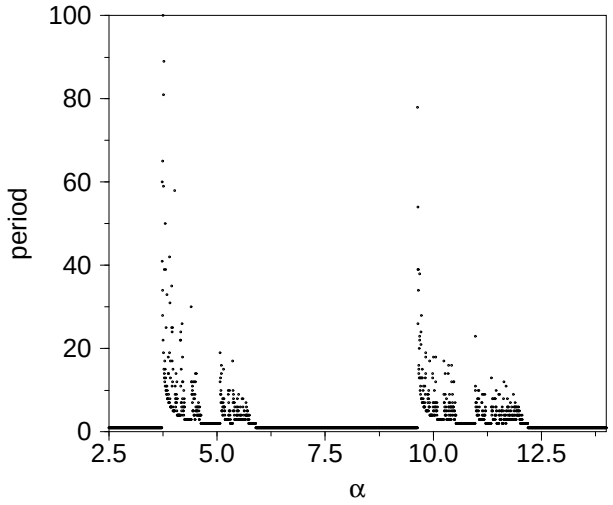

Fig. 3. Period of trajectories originally starting in the absorbing region as function of α.

1 that extend beyond $(2n+1)\pi$ because of the existence of stable periodic orbits outside the locking region; the stepwise decrease of the number of subsequent reflections at the first branch as α increases, and a high periodicity in between these subsequent plateaus; the period–doubling sequence at the left end of the period–1 plateaus (due to the finite resolution in α only the 2– and 4–cycles can be seen. The 3–cycle lies beyond the period–doubling sequence). At the edges of plateaus of periods larger than one, period-doubling bifurcations and saddle-node bifurcations can also be seen. The reason is that powers of the map have properties similar to the ones of the map itself. Fig. 3 therefore has similar structures on all scales. This type of fractal dependence of the period of a trajectory on the system parameter is also found for a particle bouncing on a vibrating platform [7].

4 The Partially Inelastic Particle

The dynamics of the partially elastic particle ($0 < \eta < 1$) show a very intricate structure. The particle velocity is no longer determined by the phase of the last reflection, and phase space becomes therefore larger. Consequently, we do now also observe chaotic orbits, in addition to periodic orbits and chattering orbits. "Chattering" means that the particle undergoes an infinite number of

reflections at the same wall during a finite time interval thereby loosing all its kinetic energy with respect to the wall. The latter is also a periodic orbit, and it is the equivalent of a locking orbit in the completely inelastic case. In the following subsections we discuss all these phenomena and the interplay between them as the parameter values are varied.

4.1 Chattering

When the particle hits the wall with sufficiently small relative velocity, it is reflected infinitely often from that wall during a finite time interval and looses all its energy, as described for the vertically shaken particle [8]. It subsequently sticks to the wall until the phase is $\phi = 0$, and then leaves the wall with relative velocity $u = 0$. Of course, in reality a collision takes a nonvanishing time, and it is therefore impossible to have an infinite number of reflections during a finite time interval, but when the collision time is much smaller than the period of the container oscillation, the number of subsequent reflections at the same wall can be very large. More importantly, as a result a "permanent" contact is made between the wall and the particle, which lasts until the acceleration of the wall reverses its sign.

In order to understand the chattering phenomenon, let us consider first a particle colliding with a wall that is accelerated at a constant rate a. This situation is equivalent to a ball bouncing in a gravitational field, where it experiences a constant acceleration toward the ground. If the initial relative velocity of the particle is u_0, the relative velocity becomes zero after the time

$$T = 2\eta u_0/a + 2\eta^2 u_0/a + ... = 2u_0\eta/a(1-\eta)$$

after the first collision. In our system, the wall acceleration is of the order $A\omega^2$, and chattering can occur if the time T is no larger than of the order of the oscillation period ω^{-1}, leading to the condition $u_0 < A\omega(1-\eta)/\eta$ for chattering. For η close to 1, u_0 must be very small, which is only possible if the particle hits the wall at a phase ϕ_0 within a distance $\Delta\phi_0 \propto \sqrt{1-\eta}$ of π, or, equivalently, if the particle's trajectory hits the (absolute) position $x = 0$ (or $x = L$) within a time interval of the order $\Delta t \sim u_0 \Delta\phi_0 \propto (1-\eta)^{3/2}$. The phase space volume $u_0\Delta t$ for which chattering occurs shrinks consequently as $(1-\eta)^{5/2}$, when η approaches 1.

The authors of [8] believe that chattering is the generic fate of a particle bouncing on a vibrating platform, just as in the completely inelastic case, with the number of reflections between two chattering events diverging as η approaches 1. In our system, however, a particle that leaves the wall at phase $\phi = 0$ and with relative velocity $u = 0$, returns to the chattering region only for certain combinations of α and η, and is otherwise trapped on a periodic or chaotic orbit. Even in those cases where a chattered particle is chattered again, there may exist other trajectories that never enter the chattering region.

4.2 Shrinking of Phase Space Volume, and Periodic Orbits

Due to dissipation, a given phase space volume shrinks with time. In particular, regions with large initial velocity are depleted, since the energy of a particle decreases exponentially fast until it reaches the regime where the time between impacts is of order unity, i.e. where its velocity is of order α. The change of u with the impact number n is approximately given by

$$\mathrm{d}u/\mathrm{d}n = -u(1-\eta)\,.$$

Using the relation $\mathrm{d}\phi \simeq (\alpha/u)\mathrm{d}n$, we find

$$u \simeq \frac{\alpha}{(1-\eta)(C+\phi)} \tag{8}$$

for the decrease of u with ϕ, with a constant C that is determined by the initial conditions. A small initial velocity interval consequently increases rapidly with increasing ϕ, leading to a strong shear of an initial domain of phase space, and interweaving different domains of attraction, as we shall see below. In fact, every domain of attraction contains points with arbitrarily large velocity.

Another consequence of the shrinking phase space volume is that all stable periodic orbits are attractive. It can easily be shown that the product of the two eigenvalues of the stability matrix is $\lambda_1\lambda_2 = \eta^2$, leading to $|\lambda_i| = \eta < 1$. In the following, we derive conditions for the existence and stability of periodic orbits of period one. Writing

$$\rho = (2n-1)\pi\frac{1+\eta}{1-\eta} \tag{9}$$

with some positive integer n, these fixed points are given by

$$\sin\phi = \frac{2\alpha - \rho\sqrt{4+\rho^2-\alpha^2}}{4+\rho^2} \quad \text{and} \quad u = \frac{2\eta}{1-\eta}\cos\phi\,. \tag{10}$$

A stable fixed point can vanish by merging either with an unstable fixed point, or it can become unstable. The merging of stable and unstable fixed points occurs when the square root in (10) becomes imaginary, leading to the condition

$$\eta > \frac{\sqrt{\alpha^2-4} - (2n-1)\pi}{\sqrt{\alpha^2-4} + (2n-1)\pi} \tag{11}$$

for the existence of the fixed point. On the other hand, a stability analysis gives a stable fixed point for

$$-\frac{1+\eta}{1-\eta}\frac{2}{(2n-1)\pi} < \tan\phi < \frac{1-\eta}{1+\eta}\frac{2}{(2n-1)\pi}\,. \tag{12}$$

The violation of the left–hand side of condition (12) corresponds to a period doubling bifurcation (one eigenvalue becomes -1), the violation of the right–hand side corresponds to a saddle–node bifurcation (one eigenvalue becomes $+1$).

4.3 Period Doubling and Strange Attractors

As we have seen in Section 3, every trajectory is periodic for $\eta = 0$ and may or may not go through the chattering region $\phi \in [\pi, 2\pi[\bmod 2\pi$. Both types of orbits can coexist for small η if the trajectory that starts in the chattering region is not trapped by the other periodic orbit. Since the basins of attraction of the chattering orbit and the normal periodic orbit are strongly interwoven, a small change in η can induce or remove such a trapping. When η is increased, normal periodic orbits typically go through a period–doubling scenario and then become a strange attractor. This attractor may be a global attractor, or it may coexist with other attractors, e.g., periodic orbits. Due to the large dissipation, the attractors are rather flat and seem almost one–dimensional in Poincaré–like plots, as also known from other systems with large dissipation, like the Lorenz attractor [11]. Fig. 4 shows the strange attractor for $\alpha = 10$ and $\eta = 0.142$. The

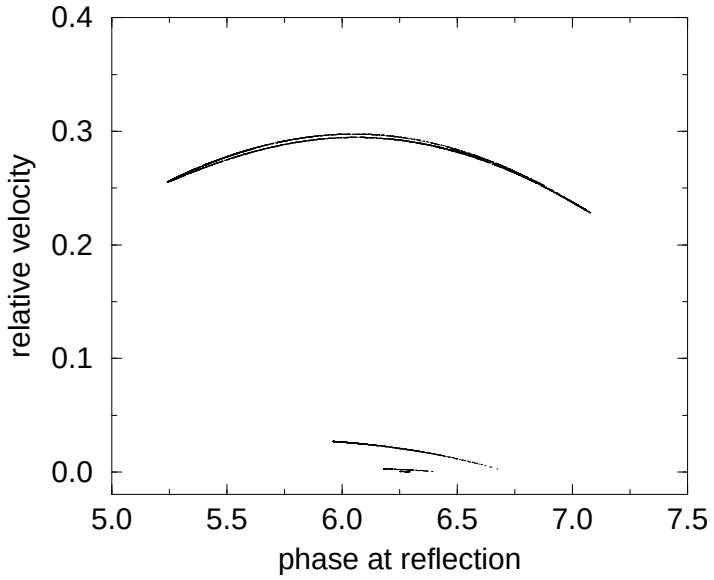

Fig. 4. The strange attractor for $\alpha = 10$ and $\eta = 0.142$.

lower arches of the attractor correspond to the second, third, and fourth reflection at the same wall and are not present for smaller η. When η increases further, the number of arches diverges, and the attractor is replaced by a chattering orbit.

As in the Feigenbaum scenario, one can distinguish intermittent periodic regimes that undergoes in turn a period–doubling scenario. Even after the attractor has been destroyed due to chattering, such intermittent periodic regimes and subsequent period–doubling cascades can still be observed when η is further increased. The strange attractor emerging from this last period-doubling

sequence is not destroyed by being chattered, but because its edge points approach an unstable periodic orbit that ultimately diverts the trajectory from the attractor and leads it on a periodic orbit.

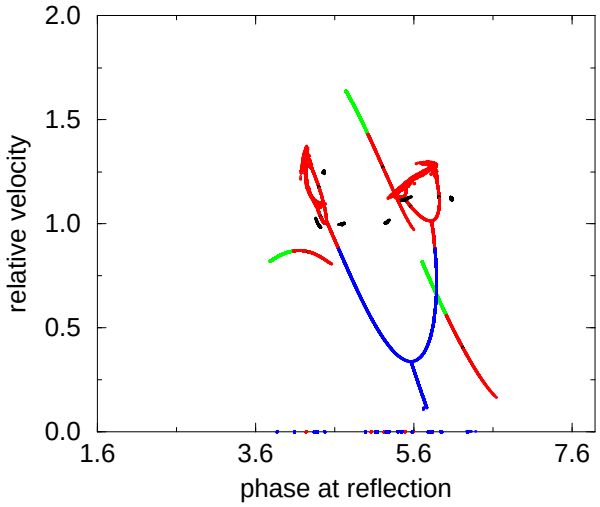

Fig. 5. The set of attractors for $\alpha = 2$ as η changes from 0 to 1. The colour changes are at η =0.5208, 0.6825, 0.6888, 0.7992.

For other values of α, different scenarios may occur. There may be several period doubling cascades, which can occur for increasing as well as decreasing values of η. Period–doubling cascades for increasing η are usually initiated by an eigenvalue of the stability matrix of a periodic orbit becoming equal to -1, while cascades for decreasing η occur when a periodic trajectory starts to experience several reflections at the same wall. Moreover, there can be intervals of η for which all trajectories experience chattering, i.e., where the only attractor is the periodic orbit with chattering. Period–doubling cascades are also observed when α is varied for fixed η. Figure 5 shows the various attractors for $\alpha = 2$ as η is increased from 0 to 1. Different colours indicate different intervals of η values. Increasing η from zero (blue part), we see a stable fixed point emerging from the chattering domain which dominates the dynamics at $\eta = 0$. This fixed point undergoes a complete period doubling scenario as η increases further. At the end of the period doubling scenario we have a chaotic attractor which continues to grow until it disappears when the particle trajectory becomes chattered. The latter part of the period doubling scenario exists simultaneously with the stable three–cycle that is also shown in the figure (red part). This three–cycle moves to the left as η increases, and it survives to $\eta = 1$ (green part). Close to $\eta = 1$, more periodic orbits exist that are not shown in the figure. Moreover, there are other small attractors which appear for intermediate values of η (the black "dust" in

the figure).

4.4 Ghost Attractors and Domains of Attraction

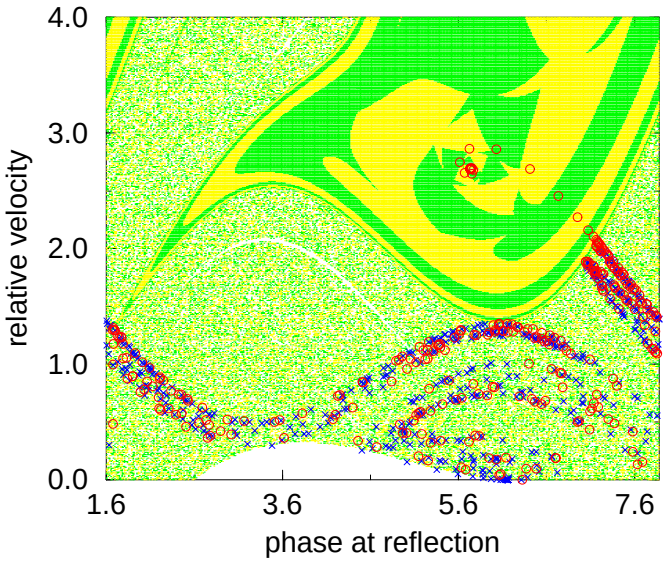

Fig. 6. The two domains of attraction for $\alpha = 10$ and $\eta = 0.61578$. The attracting fixed point is at $\phi \approx 5.7$ and $u \approx 2.7$. The domain of attraction of the fixed point is yellow and green, the domain of attraction of the chattering orbit is white. The red circles and blue crosses indicate two nearby trajectories.

Since the size of strange attractors increases with increasing η until they become absorbed by the chattering orbit, strange attractors become rare for higher values of η. Nevertheless, the "ghosts" of these attractors still continue to influence the dynamics by trapping trajectories for a transient time, which can last several hundred or thousand reflections. Consequently, the domains of attraction for normal periodic and chattering orbits become strongly interwoven, as shown in Fig. 6 for $\alpha = 10$ and $\eta = 0.61575$. There is a fixed point sitting in the center of the curl, and there is a chattering orbit. White dots belong to trajectories that will become chattered, yellow and green dots will become attracted to the fixed point and reach some small neighbourhood after and even resp. odd number of reflections. The large yellow and green areas belong completely to the domain of attraction of the fixed point, the white areas belong to the domain of attraction of the chattering orbit. For two nearby starting points in the region with the irregularly spaced green, yellow, and white dots, the trajectories follow a "ghost attractor", by which they are trapped for quite some time. The release

of the trajectories to either the attracting fixed point or the chattering domain is seemingly random due to the influence of the attractor, as can be seen from the blue and red trajectories. Since the two domains of attraction are so strongly interwoven in this region, a small change in η or α can change the fate of the trajectory that starts in the chattering region and can either lead this trajectory back to the chattering region, or to the periodic orbit. When the trajectory returns to the chattering region, the period depends strongly on the parameter values, as in the completely inelastic case. Ghost attractors similar to the one in Fig. 6 are also observed in the case of a vertically shaken particle and trap the chattering orbit for a long time [6].

5 Conclusion and Outlook

In this article, we have shown that a particle in a horizontally shaken box has a very rich behaviour. While chattering, i.e., the loss of all kinetic energy during a finite time, may occur for any value of the coefficient of restitution smaller than one, other scenarios like period–doubling and strange attractors are observed as well. The interplay between chattering, periodic, and chaotic orbits has rarely been studied before. One example is the forced oscillator impacting on a wall [12].

We have not discussed the case of a completely elastic particle. For $\eta = 1$, no energy is dissipated during a reflection, and phase space volume is perserved. Consequently stable periodic orbits are neutrally stable (i.e. both eigenvalues of the stability matrix are equal to one), and chaotic regions occupy a nonvanishing phase space volume [13, 14, 15, 10].

We have also neglected the influence of friction between the particle and the container bottom. Particles that are so slow that they cannot reach the other wall become trapped in the region between the walls, where they perform a low–amplitude periodic oscillation. trajectories. This will in particular affect long orbits like chattering orbits and strange attractors. For sufficiently large container sizes, this is the fate of all particles [10].

When $N > 1$ particles are placed in the container, new phenomena will arise. Three or more particles with a sufficiently small coefficient of restitution $\eta < 1 - 1/N$ are known to undergo an *inelastic collapse*, where they loose all their relative kinetic energy due to infinitely many collisions during a finite time [16, 17], a phenomenon similar to chatter. But even for parameter values that do not allow for an inelastic collapse, clustering phenomena occur. The Chicago group [18] studied a system with one elastic and one thermally moving wall for approximately ten particles. Most of the particles form a cluster almost at rest, while a few remaining particles travel between the boundaries at a much higher speed. We have seen a slightly different phenomenon in the periodically shaken box, namely the formation of two clusters travelling between the boundaries and the center of the system, similar to Newton's cradle.

Acknowledgements

We thank D. Wolf for helpful discussions. This work was supported by EPSRC Grant No. GR/K79307.

References

1. Straßburger, G., Betat, A., Scherer, M.A., Rehberg, I.: in *Traffic and Granular Flow*, Wolf, D.E., Schreckenbach, M., and Bachem, A. (eds.) (World Scientific, 1996)
2. Ristow, G.H., Straßburger, G., and Rehberg, I.: Phys. Rev. Lett. **79**, 833 (1997)
3. Melo, F., Umbanhowar, P., Swinney. H.L: Phys. Rev. Lett. **72**, 172 (1994); *ibid* **75**, 3838 (1995)
4. Umbanhowar, P., Melo, F., Swinney, H.L.: Nature **382**, 793 (1996)
5. Clement, E. et al.: Phys. Rev. E **53**, 2972 (1996)
6. Kowalik, Z.J., Franaszek, M., Pieranski, P.: Phys. Rev. A **37**, 4016 (1988)
7. Mehta, A., Luck, J.M.: Phys. Rev. Lett. **65**, 393 (1990)
8. Luck, J.M., Mehta, A.: Phys. Rev. E **48**, 3988 (1993)
9. De Oliveira, C.R., Gonçalves, P.S.: Phys. Rev. E **56**, 4868 (1997)
10. Drossel, B., Prellberg, T.: submitted to European Physical Journal B
11. For an beautiful introduction to the Lorenz and other strange attractors see e.g. the chapters 9 to 12 of Strogatz, S.H.: *Nonlinear Dynamics and Chaos* (Addison–Wesley, Reading, MA, 1994)
12. Budd, C., Dux, F., and Cliffe, A: Journal of Sound and Vibration **184**, 475 (1995)
13. Lin, W.A., Reichl, L.E.: Physica D **19**, 145 (1986)
14. Reichl, L.E.: *The Transition to Chaos in Conservative Classical Systems: Quantum Manifestations* (Springer–Verlag, New York, 1992)
15. Fuka, M.Z.: Phys. Rev. E **51**, 1935 (1995)
16. McNamara, S., Young, W.R.: Phys. Fluids A **4**, 496 (1992)
17. Zhou, T., Kadanoff, J.P.: Phys. Rev. E **54**, 623 (1996)
18. Du, Y., Li, H., Kadanoff, L.P.: Phys. Rev. Lett. **74**, 1268 (1995)

This article was processed using the LaTeX macro package with LLNCS style